Regular Article

ANALYTICAL
AND BIOANALYTICAL
CHEMISTRY
RESEARCH

Published by the
Iranian Chemical Society

Impact of Influencing Parameters on the Adsorption of Nickel by Kaolin in an Aqueous Medium

Toufik Chouchane* and Atmane Boukari

Research Center in Industrial Technologies CRTI, P. O. Box: 64, Cheraga 16014 Algiers Algeria

(Received 20 January 2022 Accepted 8 June 2022)

In this study, nickel elimination per kaolin from Guelma/Algeria in aqueous media was examined by applying several parameters, namely the agitation speed, pH, temperature, particle size of the solid and initial concentration. The physico-chemical investigations accomplished indicated that the kaolin in the majority is composed of silica (46.58%) and alumina (36.82). The measured specific surfaces of the raw and activated kaolin samples are respectively 98 m^2 g^{-1} and 310 m^2 g^{-1}. The pH value corresponding to the PZC is around 3.1. The adsorption capacity is measured after 60 min of stirring under specific conditions, namely V_{ag}: 150 rpm; pH: 4.3; T: 20 °C; Øs: 200µm corresponds to 45.39 mg g^{-1}. The study of the adsorption isotherms demonstrated that the Langmuir model was better adapted to the experimental data than the Freundlich and Temkin models. The values of the Langmuir parameter R_L, showed that the nickel adsorption process is favorable. The kinetic study has revealed that kinetics follows the pseudo-first-order model. However, a diffusion study has indicated that the transfer of nickel from the solution to the adsorbent was successfully controlled by external and intra-particle diffusion. The effect of temperature has indicated that this adsorption is physical, spontaneous ($\Delta G° < 0$), exothermic ($\Delta H° < 0$) and less entropic ($\Delta S° < 0$). The nickel desorption from charged kaolin is more efficient using hydrochloric acid at 0.1 M as the eluent. Considering the determined results, we estimate that kaolin from Guelma/Algeria, can be valued as a reliable, efficient and economical adsorbent for the elimination of nickel from wastewater.

Keywords: Kaolin, Nickel, Removal, Adsorption, Kinetics, Adsorption isotherms

INTRODUCTION

Water is a fundamental resource that participates strongly in the survival of man and his environment, in addition, it plays a decisive role in the evolution of current societies [1]. Its pollution by toxic elements constitutes a grave menace for humanity and the whole of society [2]. Indeed, it was found that the natural waters which are becoming increasingly restricted are mostly contaminated by toxic pollutants [3], where metal ions are most predominant [4]. Indeed, the contamination generated by metal ions is one of the principal ecological preoccupations because of their harmfulness, their accumulation in the food

chain and living organisms, and their continuous presence in nature [5]. Faced with this unfavorable situation, it was essential to propose solutions and suggest reliable and effective techniques in order to solve the problem at least partially [6]. At present, the process of treating wastewater containing toxic metals includes ion-exchange [7], solvent extraction [8], reverse osmosis [9], ultrafiltration [10] and microextraction of magnetic nanomaterials [11]. The majority of these processes produce chemical residuals and use a lot of energy. However, the adsorption phenomenon has shown more efficiency in metal ion removal processes compared to other techniques [12-14]. Indeed, it was indicated that the adsorption is a reliable technique, simple to assemble, renowned, which uses solid matter in small quantities and moreover, it offers us the opportunity to

*Corresponding author. E-mail: t.chouchane@crti.dz

recover the adsorbed metal ions [15-17].

For this reason, the adsorption process has become one of the most reliable solutions for the removal of harmful pollutants in general and metal ions in particular. Most of the materials used in this phenomenon, namely activated carbon, clays, wood waste, and sludge have provided satisfactory results.

In this sense, we used the adsorption process for the elimination of metal ions in an aqueous medium. The metal ion selected is the nickel and the adsorbent exploited is the Kaolin of Guelma, Algeria, because of its low cost and wide abundance. The main objective of this experiment was to highlight the adsorbate power of kaolin from Guelma, Algeria.

The choice of use of nickel is mainly based on its harmful and dangerous effect on humans and their environment [18,19]. Indeed, nickel has characteristics that present a potential risk to human health and ecosystems. This effect constitutes an additional major environmental problem. Persistent and environmentally mobile, its considerable utilization in commerce and industry multiplies its ability to affect and also accumulate over time [20]. The significant sources of nickel pollution are releases typically emanating from mining, forging, petroleum refining, mineral processing, electroplating, silver refining, chemical formulation, paint, battery manufacturer, vehicle emissions, municipal and industrial waste incineration disposal nickel plating and lead smelting [21,22]. The maximum permissible content of nickel in water in accordance with the World Health Organization corresponds to 5 mg l^{-1} [23];

From the literature, it was noticed that the elimination of nickel ions by the phenomenon of adsorption in solution has been the subject of several research studies [24-35]. In the majority of these works, the nickel adsorption process has been mentioned considerably favorably. As an indication, the study carried out by M. N. Zafar *et al.* [24] reported that the rice bran derivatives exhibited good adsorption capacity. where we noted that the adsorption capacities of the sodium hydroxide tetrade rice bran, the sulfuric acid tetrade rice bran, the calcium hydroxide tetrade rice bran and the hydrochloric acid tetrade rice bran corresponding respectively to 153.6, 140, 144.4 and 149.4 mg g^{-1}. Sodium dodecyl sulfate (SDS) modified grapheme oxide was favorable for the adsorption of nickel, where the adsorption

capacity was increased from 20.19 to 55.16 mg g^{-1} [26].

Kaolin is among the most abundant clays on earth, it interacts with other soil elements in contributing to the mechanical stability of the soil column, and it is structurally divided into dioctahedral and trioctahedral minerals [37]. Its structure consists of layered aluminum silicates, where the octahedral sheet of alumina (Al_2O_3) is bonded to the tetrahedral sheet of silica (SiO_2) by oxygen atoms [38]. Kaolin is used frequently in different industries, such as rubbers, paints, ceramics, plastics, cosmetics and medicaments [37].

From the literature, it was mentioned that kaolin as a solid adsorbent was often involved in the processes of removing harmful pollutants such as heavy metals [38-41], dyes [42] and organic pollutants [43]. Indeed, the unique hydrophilic surface properties of kaolin have given it a remarkable adsorption capacity [44,45]. It should be noted that this capacity could possibly be improved by specific treatment [46-50].

Studies relating to the adsorption powers of kaolin revealed that the activated kaolin was able to adsorb 46.18 mg g^{-1} of copper after 30 min of agitation [38]. Furthermore, they demonstrated the kaolin efficiency in the dye adsorption process, given that the maximum adsorption capacity of methylene blue on kaolin corresponded to 52.76 mg g^{-1} [42]. On the other hand, they evoked the contribution of kaolin as an adsorbent in suspension in the flocculation process of organic pollutants [43].

The characterization and identification of kaolin constituents have been studied using reliable physico-chemical and electronic investigations, namely X-Ray fluorescence (XRF), X-ray diffraction (XRD) and scanning electron microscopy (SEM). The specific surface was measured from the BET adsorption isotherm model.

The kinetic study was carried out under the effect of agitation, pH, temperature, particle size and initial concentration in order to optimize the process and measure the maximum experimental adsorbed capacity. The adsorption isotherms of Langmuir, Freundlich and Temkin have been applied to the experimental data to translate the nature of the adsorbate/adsorbent interaction and to define the thermodynamic equilibrium. However, adequate and commonly used kinetic models in adsorption processes such as Lagergren, Blanchard and Weber and Morris models

have been applied to the experimental results to define the order of the reaction rate and specify the mechanisms of the copper transfer from solution toward kaolin. The thermodynamic parameters were determined to explain the nature of this process under of the temperature effect. The regeneration and reuse of saturated kaolin were evaluated using several eluents.

METHODS/EXPERIMENT

Materials

The kaolin samples were taken from a clay deposit located in Guelma (eastern Algeria).

Preparation of Kaolin

The preparation and treatment of crude kaolin were realized according to the experimental protocol provided by Aroke et al. [51]. The oxidation of the organic materials and the washing and dispersion of the kaolin were carried out according to the steps given by Mustapha et al. [52]. The activation of kaolin by hydrochloric acid was carried out according to the protocol developed by de Dim et al. [53]. The treated kaolin samples were sieved to different particle sizes and preserved in desiccators. The particle size used in this work is 200, 300, 400 and 500 μm.

Analytic Methods

The physicochemical analyzes of kaolin were done by XRF (Siemens SRS 3000) and XDR (Rigaku Ultim IV). The morphology of the kaolin samples was observed using a scanning electron microscope SEM (Zeiss EVO MA25). Nickel concentration was measured using atomic absorption spectroscopy (Perkin Elmer 3110). Reagents including phosphoric acid, sodium hydroxide, hydrochloric acid, acetic acid and potassium iodide (Merck) were utilized in the treatment of crude kaolin and in the nickel desorption from charged kaolin.

Batch Adsorption Experiments

Several experiments were realized in static mode to study on the one hand the influence of pH, temperature, particle size and initial concentration on the efficiency of nickel removal by kaolin. On the other hand, to define the appropriate isotherm model, the adequate kinetics and the nature of the process.

The experimental protocol results in the addition of 1 g of kaolin prepared in a beaker of volume 1 l containing nickel solution. The nickel solutions were prepared from nickel nitrate ($Ni(NO_3)_2$, $6H_2O$). The stirring and the temperature of the solution were ensured respectively by a mechanical stirrer and a water bath fitted with a thermostat. The elimination process was realized by taking 5 ml samples every 10 min of stirring. The nickel absorption kinetic was studied on 04 similar workstations. The number of samples taken at each station is 3. It is important to note that the 04 stations started at the same time.

The operational approach applied was to take 3 samples from each station, i.e. 12 samples of each series. For studying the contact time effect, the sampling of the first series has started respectively from 10, 40, 70 and 100 minutes of agitation (station1: 10, 20, 30 min, station 2: 40, 50, 60 min, station 3: 70, 80, 90 min and station 4: 100, 110, 120 min). After 120 min of stirring, we stopped the manipulation, changed new solutions and we did the same thing again, with the difference that the sample takings started after 130 min of stirring (station1: 130, 140, 150 min, station 2: 160, 170, 180 min, station 3: 190, 200, 210 min and station 4: 220, 230, 240 min). For the study of the effect of pH, temperature and grain size, we worked with a single series (station1: 10, 20, 30 min, station 2: 40, 50, 60 min).

This experimental protocol was chosen to maintain the same initial concentration and also to ensure the continuity of the study.

The nickel adsorbed capacity at equilibrium and at time t was calculated from the following equations:

$$q_e = \frac{C_0 - C_e}{m} \times V \tag{1}$$

$$q_t = \frac{C_0 - C_t}{m} \times V \tag{2}$$

where C_0 is Initial concentration (mg l^{-1}); C_e is concentration at equilibrium (mg l^{-1}), C_t is concentration at time t (mg l^{-1}), V is the volume of the solution (l) and m is the mass of adsorbent (g).

The parameters which were used in this process are: the

initial concentration (C_0), the agitation speed (V_{ag}), the hydrogen potential (pH), the temperature of the solution (T) and the particle size of the solid ($\varnothing_S$).The experimental conditions used in this work are as follows.

• Equilibrium time: C_0: 30 mg l^{-1}; V_{ag}: 150 rpm; pH: 5,4; T: 20 °C; $\varnothing_s$: 400 µm, M: 1 g, V: 1 l.

• pH optimization: C_0: 30 mg l^{-1}; V_{ag}: 150 rpm; pH: 2.5, 4.3 and 5.4; T: 20 °C; $\varnothing_s$: 400 µm, M: 1 g, V: 1 l.

• Temperature optimization of: C_0.: 30 mg l^{-1}; V_{ag}: 150 rpm; pH: 4.3; T: 20, 30, 40 and 50 °C, $\varnothing_s$ = 400 µm. M: 1 g, V: 1 l.

• Granulometry optimization: C_0: 30 mg l^{-1}; V_{ag} 150 rpm; pH: 4.3; T: 20 °C; $\varnothing_s$: 100, 200, 300 and 400 µm, M: 1 g, V: 1 l.

• Adsorption capacity: C_0: 10-80 mg l^{-1}; V_{ag}: 150 rpm; pH: 4.3; T: 20 °C; $\varnothing_s$: 200 µm, M: 1 g, V: 1 l.

Specific Surface Measurement

The surface areas of raw and activated kaolin samples were measured from the amount of nitrogen adsorbed in relation to its pressure at the boiling temperature of liquid nitrogen and under normal atmospheric pressure. The isotherm data for nitrogen gas desorption at 77 K were analyzed with the Brunauer, Emmett et Teller model (model BET) [54].

Point of Zero Charge

The point of zero charge is the pH value of the solution when the sum of positive charges and negatives are equal on the superficial surface, that is, the charge is zero [55]. From the literature, when the pH < pHzpc, the kaolin surface turns positive which favors anionic ions. On the other hand, when the solution pH > pHzpc, becomes again negative, which favors cationic ion adsorption [56,57]. The point of zero charge is determined by the procedure presented by P. Chutia *et al.* [58].

Nickel Desorption

The amount of saturated kaolin that was utilized in this process is 20 g. The saturated kaolin recovered after filtration and was dehydrated at 105 °C for 48 h. Desorption was accomplished using distilled water and different eluents, namely sulfuric acid (0.1 N), nitric acid (0.1 M) and hydrochloric acid (0.1 M). The used volume is 1 l. The

nickel(II) quantity desorbed was measured with an atomic adsorption spectrometer.

RESULTS AND DISCUSSION

Characterization of Kaolin

Identification of the constituents of the kaolin samples and their morphologies were obtained after grinding, sieving and dehydrating under a vacuum at 105 °C for 12 h. Following previous studies [38,59] and on the basis of new investigations, the kaolin samples under examination kept the same composition and the morphology study kept the same morphology (Figs. 1 and 2) (tab 1). Indeed, the analyzes performed by XRF and XRD indicated that kaolin consists mainly of silica (SiO_2: 46.58%), alumina (Al_2O_3: 36.82) and a minimum percentage of oxides. The morphology of the raw kaolin and activated were determined by scanning electron microscope (Fig. 2). In the first micrograph (Fig. 2a), the existence of a smooth surface was observed, generated by the development of several sheets stacked in the form of agglomerates. On the other hand, on the second micrograph (Fig. 2b), the existence of a more porous structure was noticed, caused by the emergence of other sites and also it was observed the expansion of the surface under the effect of hydrochloric acid [56,60].
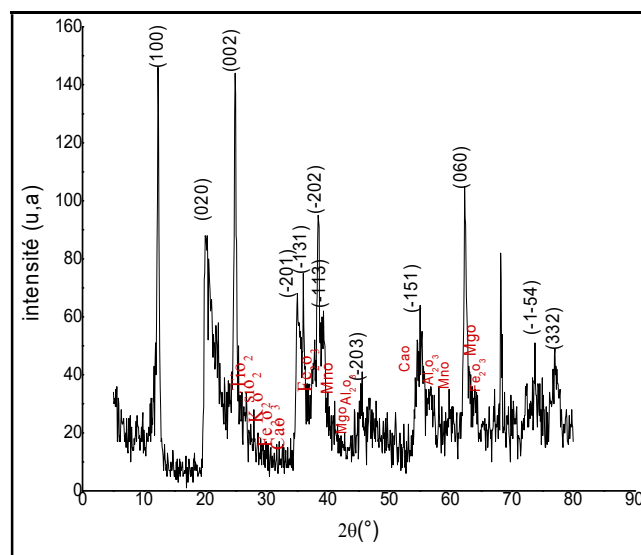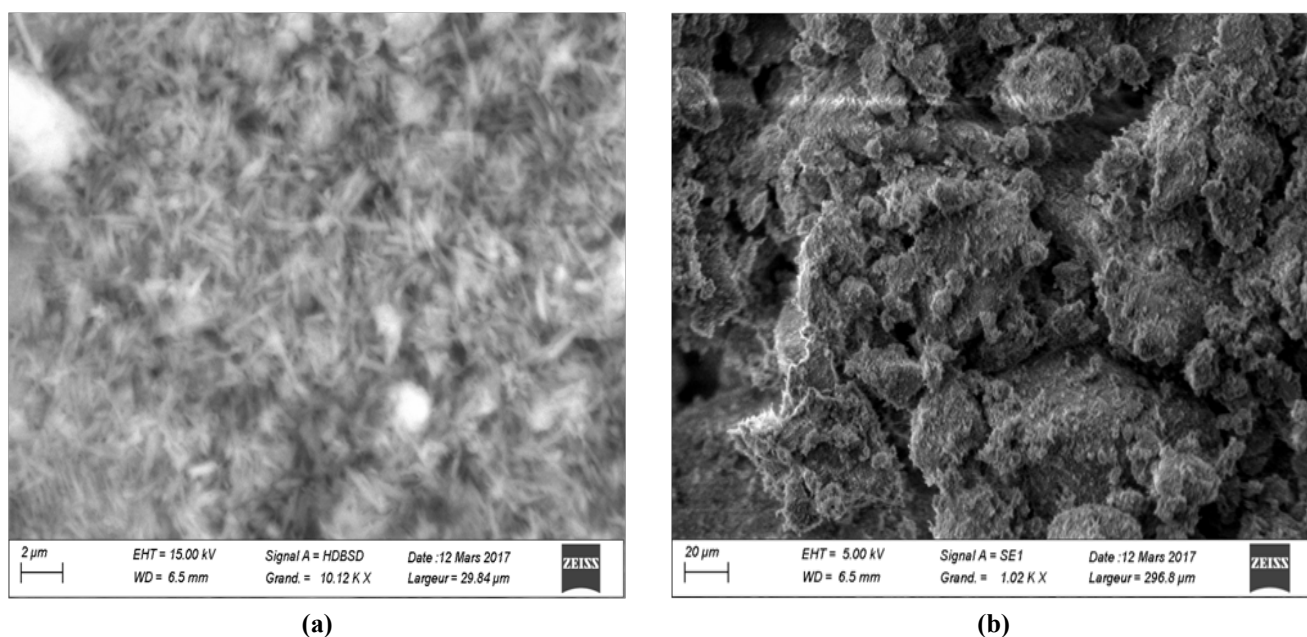

Fig. 1. Diffractogram of raw kaolin [48].

Fig. 2. (a) SEM picture of raw kaolin [48], (b) SEM picture of activated [48].

The activation of clays by acids is a very important and frequently applied approach, because it positively influences the superficial surface of the solid by multiplying the adsorption sites, which translates into better adsorption [61,62]. Indeed, the measured specific surfaces of the raw and activated kaolin samples are respectively 98 m^2 g^{-1} and 310 m^2 g^{-1}. This multiplication of active sites is surely due to several factors, namely the elimination of impurities, the substitution of metal ions by hydrogen ions and the generation of silica [53].

Under the operating conditions established by and with our sample, the measurement data showed that the pzc is at around 3.1

Adsorption Study

 Effect of agitation time. The evaluation of contact time in adsorption processes is an essential step, because it allows us to define the equilibrium time and thus the saturation of the adsorbent under very specific experimental conditions [63].

The effect of contact time showed that the adsorption process was prompt over the first 40 min and then it started to decrease with time before being non-existent after 60 min of agitation (Fig. 2). Indeed, the strong adsorption in the first step has been due to the rapid transfer of nickel ions from the adsorbate to the external surface of the kaolin (external diffusion). On the other hand, in the second step, the decrease in the adsorption rate was due to the slow diffusion of the nickel ions from the external surface to the interior of the pore (internal diffusion). From these experimental data, it was noticed that increasing the contact time from 60 to 240 min had no effect on the adsorption process (Ce = cst). This finding led us to assume that the kaolin has reached the saturation stage. Therefore, we estimated 60 min as the equilibrium time of nickel adsorption on kaolin under our experimental conditions.

According to the literature, it was mentioned that kaolin from Gbako Local, Nigeria gave a better equilibrium time during the removal of Cr, Cd and Zn (15 min) [52]. Moreover, the equilibrium time measured during the adsorption of Cu and Zn by kaolin from Guelma, Algeria was 30 min [38,59]. These performances encourage us to further improve the treatments carried out on the kaolin to achieve a better equilibrium time.

 Effect of pH. From the research work realized, it has been mentioned that the pH of the solution occupies a considerable role in the adsorption processes. This importance is aroused by the influence of pH on the surface

properties of the adsorbent and on the character of the metal ions in the solution [64-66]. In this part, we have tested the adsorption process in three different media, namely pH 2.5, pH 4.3 and pH 5.4 (Fig. 4).

The effect of pH 2.5 has shown that the nickel adsorption on kaolin is unfavorable (Fig. 4). Indeed, for strongly acidic media (pH 2.5), the effect of the competition generated by the excess protons reduces the transfer of nickel ions from the solution to the adsorbent [67] and in addition, the pH of the solution is lower than PZC (pH < pHpzc) [56].

Subsequently, a remarkable increase the adsorption efficiency was observed, in particular at pH 4.3. As a result, the maximum quantity adsorbed and the rate of adsorption increased from 7.81 to 23.15 mg g^{-1} and from 26.03 to 77.17% (Fig. 3). For this particular case, the pH of the solution was higher than PZC (pH > pHpzc), indicating that the negatively charged adsorbent surface was attractive for positively charged nickel metal ions (attractive interaction effect) [68]. This result confirms the favorable effect of pH on the surface properties of the adsorbent.

On the other hand, at a pH equal to 5.3, a decline in the efficiency of the adsorption process was observed, where the adsorption yield fell from 77.39 to 57.86%. This effect was probably caused by the precipitation of nickel ions due to the presence of hydroxide ions in the solution [69]. In conclusion, we estimated that the optimal pH is equal to 4.3.

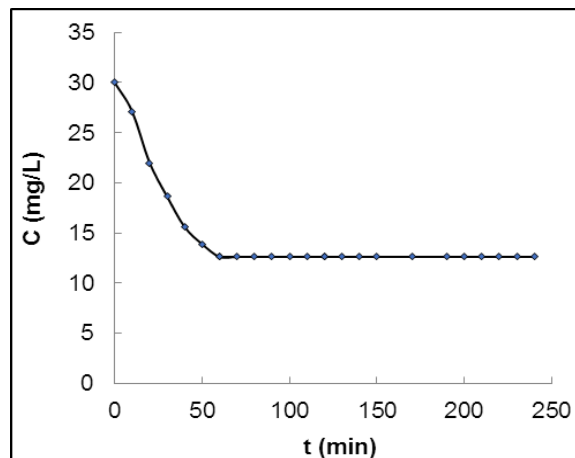**Effect of temperature.** The medium temperature is a

Fig. 3. Effect of contact time.

greatly significant parameter the fact that it influences the fixation of the metal on the adsorbent by exerting a considerable power on the speed of adsorption [70-72]. In this study, the temperature impact of nickel adsorption on the kaolin surface was studied at chosen temperatures, namely 20, 30, 40 and 50 °C (Fig. 5).

From the experimental data, it was observed that the adsorption process is better at 20 °C (Fig 5a). On the other hand, it has been reported that increasing the temperature negatively influences adsorption efficiency (Fig. 5b). At this temperature (20 °C), the equilibrium concentration (Ce) and the calculated adsorption yield (R) correspond to 13.42 mg l^{-1} and 77.16%.
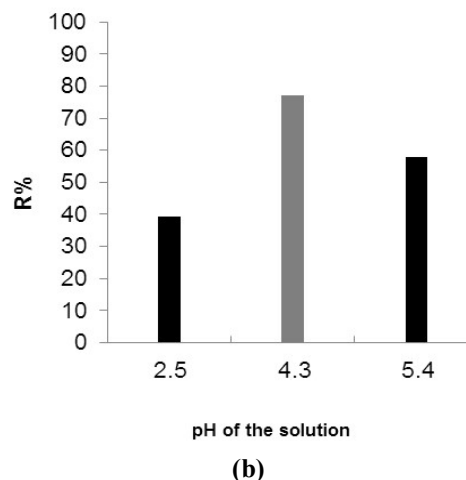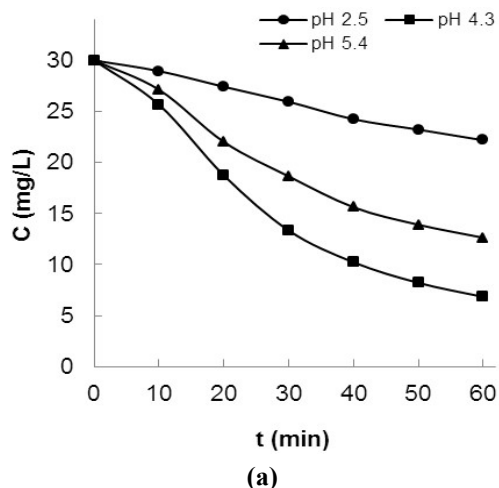

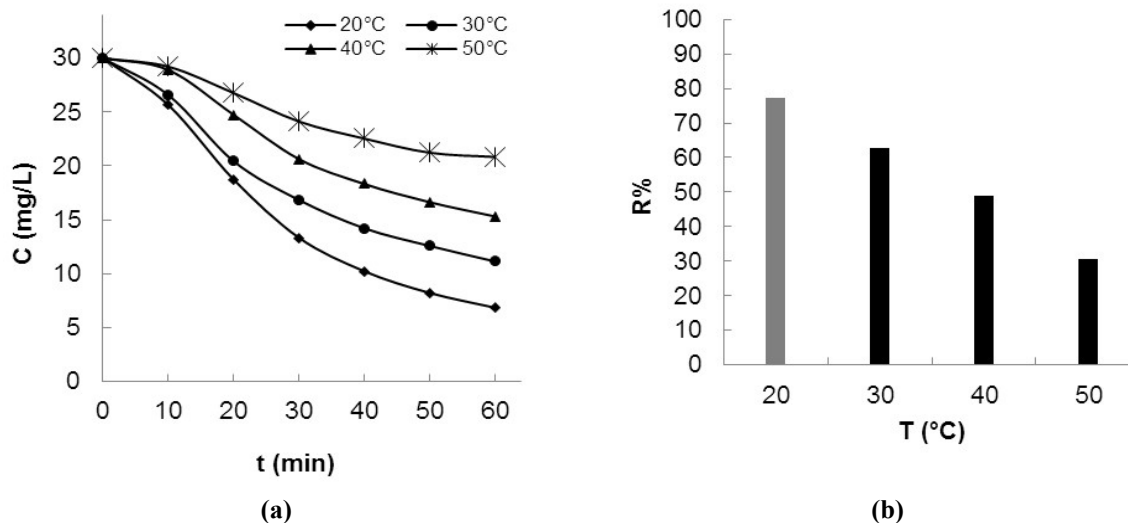**Fig. 4.** Effect of solution pH: (a) Adsorption kinetics, (b) Removal efficiency.

(a)   **(b)**

Fig. 5. Effect of the solution temperature: (a) Adsorption kinetics, (b) Removal efficiency.

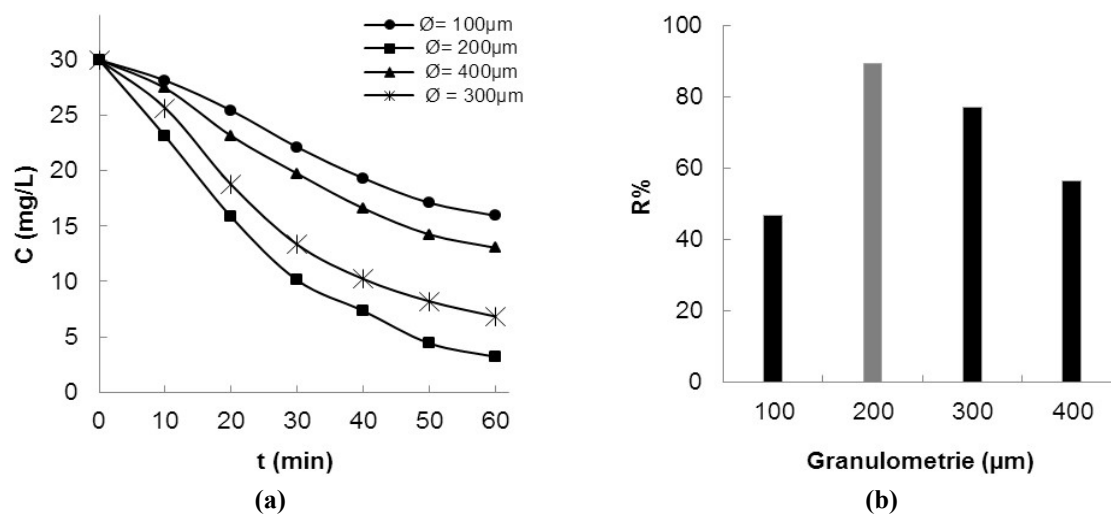**(a)**   **(b)**

Fig. 6. Effect of the adsorbent particle size: (a) Adsorption kinetics, (b) Removal efficiency.

On the other hand, the adsorption rate calculated at 30, 40 and 50 °C decreased respectively by 14.3, 28.23, 46.6% compared to the yield calculated at 20 °C (Fig. 5b). This effect was probably motivated by the increase in the opposition to mass transfer and decreased diffusion of nickel ions from the solution to the surface of the kaolin. The regression of the adsorption yield with the temperature rise led us to predict that the adsorption of nickel on kaolin is exothermic in nature [73,74]. From these results, we judged that T = 20 °C is the ideal temperature for the nickel adsorption in solution on kaolin.

Influence of particles size of kaolin. According to various research works, it has been stated that the particle size of the adsorbent has a considerable impact on the adsorption rate [75-77]. In this context, our experimental manipulations were directed to examine the utility and performance of particle size in this process. The particle size used varies from 100 to 400 μm (Fig. 6).

Following the tests realized, it was demonstrated that the nickel adsorption on kaolin is considered unfavorable in the case of particles of minimal diameter ($Ø_s$ = 100 μm) (Fig. 6). This consequence is potentially due to the

appearance of the coalescence phenomenon [38].

The experimental results specified that the nickel adsorption rate is maximum at a particle size corresponding to 200 μm. On the other hand, they demonstrated that the adsorption efficiency decreases with the increase in particle size from 200 μm (Fig. 6b). The capacities and adsorption rates for its different particle sizes correspond to 26.79 mg g^{-1}, 89.3% (200 μm), 23.15 mg g^{-1}, 77.16% (300 μm), 16.95 mg g^{-1}, 56.5% (400 μm). The regression of the adsorption rate with the increase in the size of the particles was surely caused by the narrowing of the specific surface and the reduction of the active sites of adsorption, which negatively influenced the adsorption power of the solid [78].

From this step, it was judged that the adequate and optimal particle size for better adsorption corresponds to 200 μm.

Effect of initial concentration. In this part, the effect of the initial concentration on the nickel adsorption process was studied under specific conditions, namely V_{ag}: 150 rpm; pH: 4.3; T: 20 °C; $Ø_s$: 200 μm, M: 1 g, V: 1L. The concentrations of nickel used range from 10 to 80 mg l^{-1}.

The plots of the curves of the functions qe = f (Ce) and R = (C$_0$) are presented in Fig. 7 and the results obtained from the effect of the initial concentration on the nickel adsorption process are displayed in Table 2.
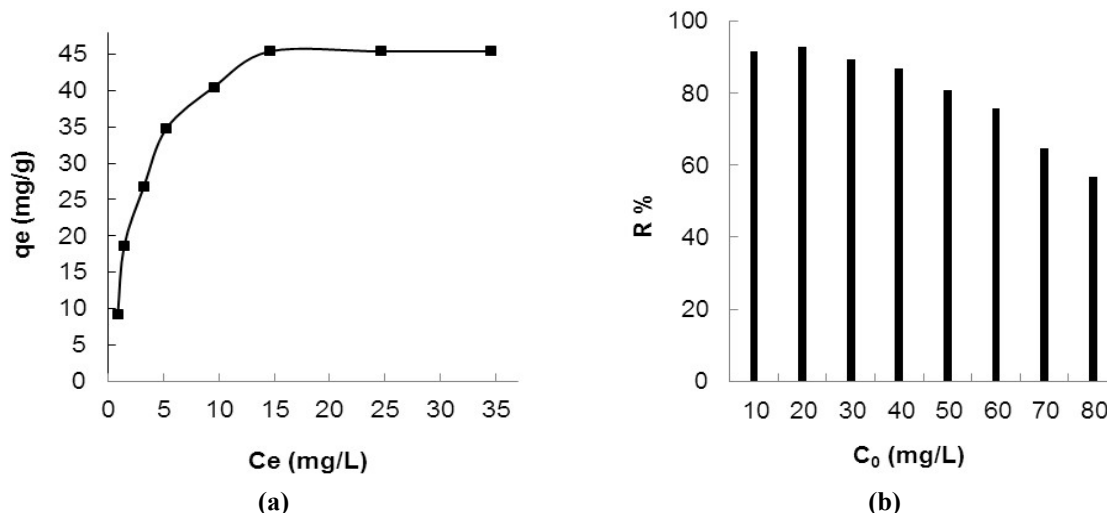
From the experimental adsorption isotherm (Fig. 7a), it was observed that the adsorption capacity increases with the increase of the initial concentration at a certain level and

Table 1. Chemical Composition of Djebel Dbagh Kaolin [48,52]

Elements	%Mass
SiO$_2$	46.58 ± 2.3152
Al$_2$O$_3$	36.82 ± 1.36
Fe$_2$O$_3$	0.78 ± 0.3327
MnO	0.14 ± 0.143
MgO	0.13±0.0665
CaO	0.21 ± 0.3327
NaO$_2$	0.18 ± 0.141
K$_2$O	0.091 ± 0.0181
TiO$_2$	0.089 ± 0.0123
LI	13.55 ± 0.845
H$_2$O	1.43 ± 0.231

then it becomes constant (60 mg l^{-1}, 46.39 mg g^{-1}) (Table 2). On the other hand, the opposite effect was observed for adsorption efficiency, where we noticed that the adsorption rate is inversely proportional to the initial concentration (Fig. 7b).

The increase in the adsorption capacity was linked to the forces of attraction which are established between the surface of the adsorbent and the nickel ions. Moreover, the regression of the adsorption percentage was caused by the limited number of active adsorption sites compared to the considerable number of available ions.

(a)   **(b)**

Fig. 7. Effect of initial concentrations: (a) Experimental adsorption isotherm, (b) Removal efficiency.

Table 2. The Data Obtained from the Effect of Initial Concentration on the Nickel Adsorption: Error in Analysis = 0.02 mg l^{-1}

C_0 (mg l^{-1})	10	20	30	40	50	60	70	80
C_e (mg l^{-1})	0.85	1.42	3.21	5.24	9.53	14.61	24.61	34.61
q_e (mg g^{-1})	9.15	18.58	26.19	34.76	40.47	45.39	45.39	45.39

Growing the initial concentration from 60 to 80 mg l^{-1} had no effect on the adsorption power of kaolin because the active adsorption sites on the surface of this solid material have been saturated. Therefore, the maximum adsorbed capacity of nickel per gram of kaolin under optimum conditions has been estimated as 46.39 mg [79-81].

Adsorption Isotherms

In order to represent the nickel adsorption process on kaolin and explicate metal ion-clay interaction, we used frequently applied models, namely the Langmuir, Freundlich and Temkin isotherms. The Freundlich model considers that the adsorption is realized on the heterogeneous surface where the distribution of active adsorption sites is not uniform (multilayer model). Its linear formula is shown below [82]:

$$\log q_e = \log K_F + \frac{1}{n} \log C_e \qquad (3)$$

The Langmuir isotherm model supposes that the adsorption is realized on the homogeneous surface in the monolayer model [83], which can be expressed in the case of adsorption in solution by the following equation:

$$\frac{C_e}{q_e} = \frac{1}{q_{max}} C_e + \frac{1}{q_{max} b} \qquad (4)$$

The Temkin model considers that multilayer adsorption concretizes particularly on a linear regression of the adsorption energy [84]. Its linear formula is shown below

$$q_e = B_T \ln A_T + B_T \ln C_e \qquad (5)$$

$$B_T = \frac{RT}{b_T} \qquad (6)$$

where q_e is adsorbed capacity at equilibrium (mg g^{-1}), C_e is the concentration of solution at equilibrium (mg l^{-1}), q_{max} is the maximum adsorbed capacity (mg g^{-1}) and b is the thermodynamic constant of the adsorption equilibrium (l mg^{-1}), K_F and 1/n are the Freundlich constants related to adsorption and affinity, A_T is Temkin isotherm equilibrium binding constant (l g^{-1}), b_T is Temkin isotherm constant, R universal gas constant (8.314 J mol^{-1} K^{-1}) T Temperature at 298 K and B_T is Constant related to the heat of sorption (kJ kmol^{-1}).

The three model presentations and their adsorption isotherms are illustrated in Figs. 8a, 8b, 8c and 9a. The parameters of these mathematical models are listed in Table 3.

According to the results obtained, it was observed that the Langmuir model is more adapted to this adsorption process than those of the Freundlich and Temkin models. This result was justified by the values of the regression coefficients and the maximum quantities adsorbed [85]. Indeed, the regression coefficient of the Langmuir model is higher than that of Freundlich and Temkin ($R^2_{Langmuir}$ = 0.99, $R^2_{Freundlich}$ = 0.85 , R^2_{Temkin} = 0.94). In addition, the maximum adsorbed capacity resulting from the Langmuir model is closest to the maximum amount adsorbed experimentally (Table 2).

This outcome showed us that the adsorbent is a monolayer with a homogeneous surface, where all of the active adsorption sites have similar relationships with nickel ions [75]. The calculated value of the Temkin model parameter (Bt = 11.41) reveals that the interaction between kaolin and nickel ions in solution is physical [86].

(a)

(b)

(c)
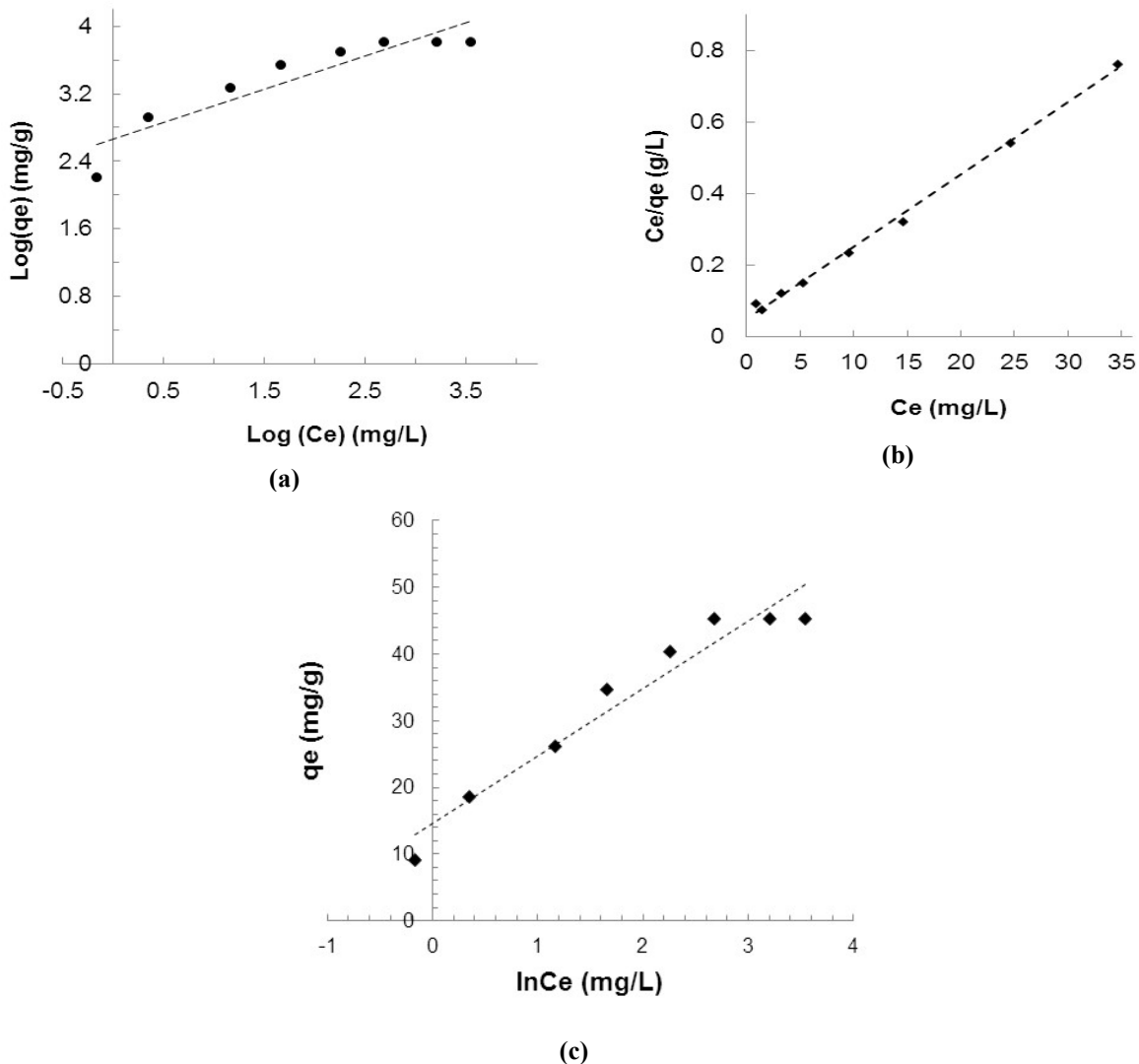
Fig. 8. (a) Freundlich model presentation, (b) Langmuir model presentation.

Table 3. Isotherm Parameters for Adsorption of Nickel by Kaolin

	K_F	n	R^2
Freundlich	$(mg\ g^{-1})\ (ml\ mg^{-1})^{1/n}$		
	14.28	2.52	0.85
Langmuir	q_{max}	b	R^2
	$(mg\ g^{-1})$	$(l\ mg^{-1})$	
	46.08	0.42	0.99
Temkin	A_T	B_T	R^2
	$(l\ g^{-1})$	$(kJ\ kmol^{-1})$	
	4.22	11.41	0.94

From Fig. 9a, we noticed that the adsorption isotherms exhibit a type L appearance. The latter is characterized by a rapid increase in the amount adsorbed in the low concentration range at equilibrium, followed by the formation of a long horizontal plateau. The elevate in the amount adsorbed is caused by a rise in the driving force of the concentration gradient. The presence of a long plateau is due to the saturation of the adsorption active sites. This result allowed us to confirm that the adsorption was realized on a homogeneous surface.

The evaluation and the favorability of adsorption can also be examined by the involvement of the R_L parameter
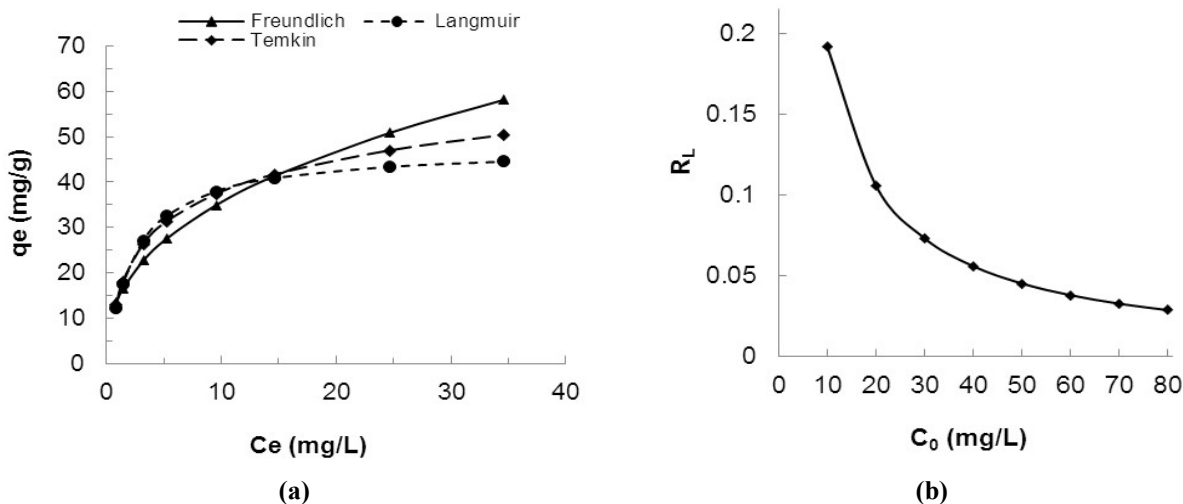
Fig. 9. (a) Adsorption isotherms presentation, (b) Evolution of R_L ration as a function C_0.

[87]. Indeed, the R_L values indicate the nature of the adsorption. Adsorption is favorable if $0 < R_L < 1$, unfavorable if $R_L > 1$, linear if $R_L = 1$, and irreversible if $R_L = 0$ [88,89].

The dimensionless parameter R_L is calculated from Eq. (7):

$$R_L = \frac{1}{1 + C_0 b} \tag{7}$$

where b is the Langmuir isotherm constant (l mg^{-1}) and C_0 is the initial concentration (mg l^{-1}).

According to Fig. 9b, it was noticed that the values of the parameter R_L decrease with the increase of the initial concentration of 0.19 and 0.02. This outcome signifies that the nickel adsorption on kaolin is favorable [90]. This conclusion is in agreement with the value of the Freundlich parameter n (n = 2.52), which considered that the adsorption was favorable [90].

Kinetics of Adsorption

In order to define the adsorption kinetics and deduce the process of the transfer of the metal ion from the solution to the adsorbent, we applied three kinetic models to our experimental data, namely the Lagergren (pseudo-first-order) [92], Blanchard (pseudo-second-order) [93], internal diffusion (Weber Morris) [94] and external diffusion. The models involved are presented by the Eqs. (8)-(11).

$$\ln(q_e - q) = -k_{Lag}t + \ln q_e \tag{8}$$

$$\frac{t}{q} = \frac{1}{k_b q_e^2} + \frac{1}{q_e} \tag{9}$$

$$q = k_w \sqrt{t} \tag{10}$$

$$\ln(C_t) = k_{ext}t \tag{11}$$

Where q_e is the adsorbed quantity at equilibrium (mg g^{-1}), q is the amount of metal ions adsorbed at time t (mg g^{-1}), Co initial concentration (mg l^{-1}), C_e is the equilibrium concentration (mg l^{-1}), C_t is the remaining concentration at time t (mg l^{-1}), t is the time of adsorption process, k_{Lag} is the constant pseudo-first-order kinetic equation (min^{-1}), k_b is the constant of pseudo-second-order speed equation (min^{-1}), k_w is the diffusion rate constant in the pores (mg m^{-1} min^{½}), k_{ext} is the external diffusion constant (mg l^{-1} min^{-1}) and C is the intercept and it's tied to the boundary layer.

The adsorption kinetics of nickel on kaolin has been studied under optimal conditions, namely C_0: 30 mg l^{-1}; V_{ag}: 150 rpm; pH: 4.3; T: 20, 30, 40 and 50 °C; Ø$_s$: 200 μm and t: 0 to 60 min.

Presentations of pseudo-first-order, pseudo-second-order, internal diffusion, and external diffusion are respectively illustrated in Figs. 10a, 10b, 11a and 11b. The parameters obtained are grouped in Table 4.
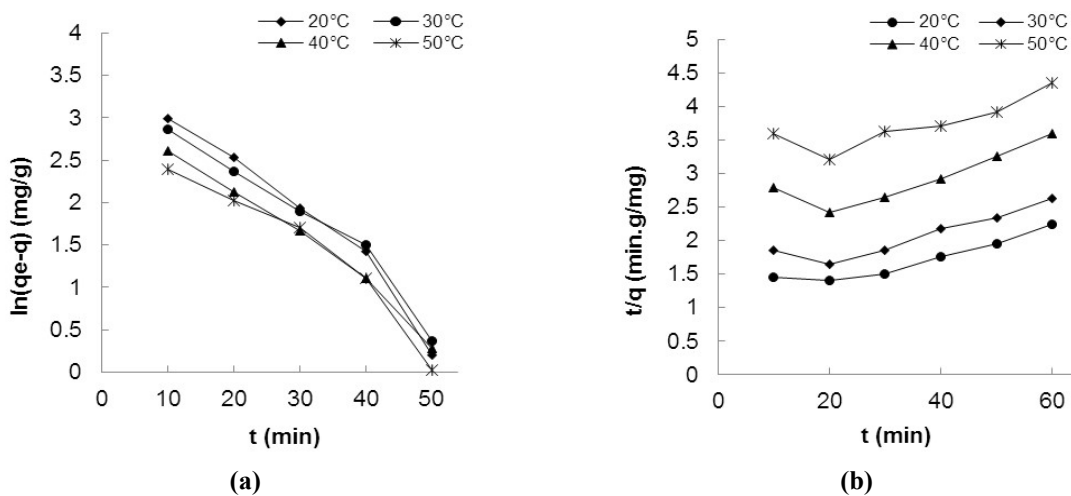
(a)

(b)

Fig. 10. (a) Pseudo first order model, (b) Pseudo second order model.

(c)
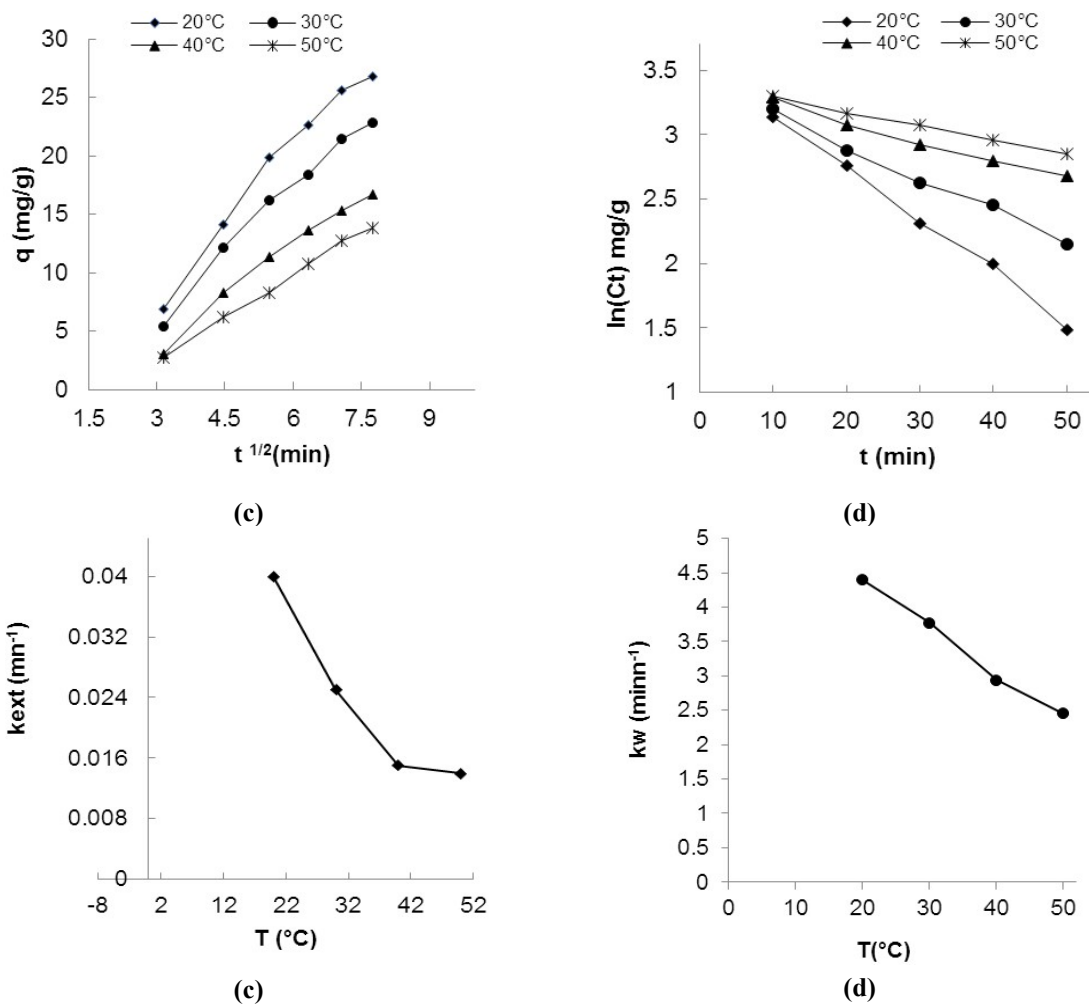
(d)

(c)

(d)

Fig. 11. (a) Intraparticle diffusion presentation, (b) External transport presentation, (c) External diffusion constant as a function of temperature, (d) Internal diffusion constant as a function of temperature.

Table 4. Pseudo First and Second Order Parameters

T		Pseudo first order				Pseudo second order	
	qe_{exp}	K_{lag}	qe_{theo}	R^2	K_b	qe_{theo}	R^2
(°C)	(mg g^{-1})	(min^{-1})	(mg g^{-1})	(%)	(g mg^{-1} min^{-1})	(mg g^{-1})	
20	26.79	0.068	26.86	0.96	8.99×10^{-4}	31.25	0.90
30	22.86	0.059	23.35	0.96	8.43×10^{-4}	28.57	0.84
40	16.68	0.052	18.82	0.98	8.58×10^{-4}	22.72	0.73
50	13.79	0.052	16.13	0.94	7.34×10^{-4}	20.83	0.70

Table 5. Parameters of Internal and External Diffusion

T		External diffusion			Intraparticle diffusion	
	$K_{ext. D.}$	Intercept	R^2	k_w	Intercept	R^2
(°C)	(min^{-1})		(%)	(mg g^{-1} min$^{-0.5}$)		(%)
20	0.04	3.561	0.99	4.4	5.82	0.97
30	0.025	3.423	0.99	3.77	5.46	0.98
40	0.015	3.4	0.98	2.94	5.43	0.98
50	0.014	3.4	0.99	2.45	4.88	0.99

From the results cited in Table 4, we observed that the correlation coefficients of the Blanchard model were inferior to that of Lagergren and in addition, theoretical adsorption capacities derived from the Lagergren model were closer to the experimental capacity. According to these results, it was considered that the adsorption of nickel on kaolin follows pseudo-first-order kinetics [95].

In order to identify the process of nickel adsorption on kaolin, it was imperative to delimit and identify the limiting stages of this phenomenon. In this sense, we studied the various limiting stages of adsorption kinetics, namely the diffusion of Ni(II) from the solution towards the boundary layer, its transfer from the boundary layer to the surface of the adsorbent (external diffusion) and its diffusion of the solute from the surface of the solid towards the inside of the pores (intraparticle diffusion).

According to Weber and Morris, the intra-particle diffusion is involved in the adsorption process if the plot of the function $q = f(t^{1/2})$ is a linear line and it controls the adsorption process if only if the line passes through the origin [96]. Otherwise, internal diffusion is not the only mechanism controlling the adsorption process [97,98].

From Fig. 10a, it was noticed that the plot of the function $q = f(t^{1/2})$ gave a linear straight line that did not pass through the origin for the different temperatures studied ($C \neq 0$). This finding lets us say that internal diffusion is not the only mechanism controlling the rate of nickel adsorption.

For further understanding of the mechanism of metal ion transport from solution to the adsorbent, we have examined the plot of the logarithm of the residual concentration as a function of time at different temperatures.

The illustrations from the function $\ln(Ct) = f(t)$ showed that all the straight lines are linear with regression coefficients greater than 90% (Table 4). These results explained to us that there was a resistance due to the boundary layer during the transfer of the metal ion from the solution to the adsorbent. This outcome leads us to suppose that external diffusion is also involved in the process of nickel adsorption on kaolin [38,99]. Therefore, it has been concluded that the overall rate of nickel adsorption is controlled by external transport as an instantaneous process followed by internal transport [100-102].

The traces of the functions $k_{ext} = f(t)$ and $k_W = f(t)$,

informed us about the mechanism of adsorption of nickel on kaolin under the effect of temperature. From Fig. 11c, It was observed that the external transport of nickel from the solution to the adsorbent is controlled firstly by the fast diffusion regime at T < 40 °C followed directly by the slow kinetic regime from 40 to 50 °C. On the other hand, from Fig. 11d, it has been indicated that the internal transport of nickel inside the surface of kaolin under the effect of temperature is limited only by the internal diffusional regime.

In both presentations, it was noticed that the rate constant (k) and the intercept (C) decreased with increasing temperature. This finding led us to assume that the rate of internal diffusion decreases with increasing temperature [103], the adsorption is rapid at 20 °C [104], and to predict that the nickel adsorption phenomenon is exothermic.

Thermodynamic Study

In order to clarify the nature of the nickel adsorption process on kaolin (spontaneous, exothermic/endothermic, random) [105], a thermodynamic study was undertaken under the effect of temperature. The distribution coefficient (K_d) was used to calculate the thermodynamic parameters from Eqs. (11)-(13) [106,107]:

$$\Delta G° = -RT \ln k_d \tag{11}$$

$$\Delta G° = \Delta H° - T\Delta S° \tag{12}$$

$$\ln k_d = \frac{\Delta H^0}{R} \times \frac{1}{T} + \frac{\Delta S°}{R} \tag{13}$$

The value of K_d is calculated from the following equation [108].

$$k_d = \frac{C_i - C_e}{C_e} \times \frac{V}{M} = \frac{q_e}{C_e} \tag{14}$$

Where ΔG is the free energy variation (kJ mol^{-1}), ΔS is the entropy variation (J mol^{-1} k^{-1}), ΔH is the enthalpy variation (kJ mol^{-1}), R is the universal gas constant (8.314 J mol^{-1} k^{-1}), T is the absolute temperature (K), k_d is the solute distribution coefficient (l g^{-1}).

ΔH is determined from the plot of the function $\ln(k_d) = f(1/T)$, ΔS is calculated from the equation 13, ΔG is calculated from the equation 12 and Ea is determined from the plot of the function $\ln(k) = f(1/T)$.

The activation energy and the thermodynamic parameters were determined under the following experimental conditions: C_0: 60 mg l^{-1}; V_{ag}: 150 rpm; pH: 4.3; T: 20, 30, 40, 50 °C; Ø$_s$: 200 μm.

The values of the thermodynamic parameters, activation energy and distribution coefficients are presented in Table 6. The plot from the logarithm of the distribution coefficient $\ln(k_d)$ as a function the inverse of the temperature (1/T) is indicated in Fig. 12.
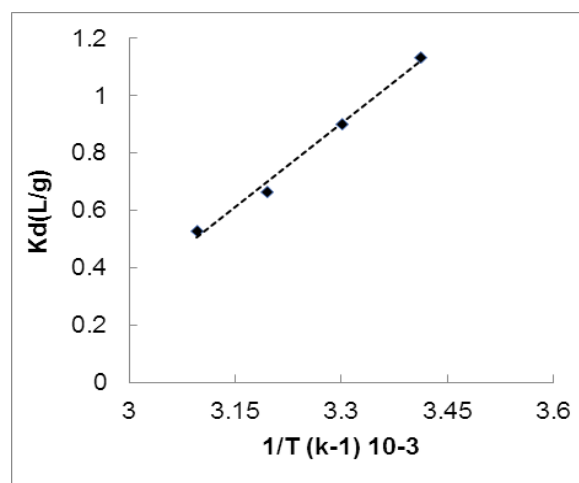

Fig. 12. Van't Hoff plot for adsorption of nickel.

Table 6. Thermodynamic Parameters

Temperature (K)	ΔH° (kJ mol^{-1})	ΔG° (kJ mol^{-1})	ΔS° (J mol^{-1} K^{-1})	Ea (kJ mol^{-1})	K_d (l g^{-1})
293		-19.55			3.10
303	-16.18	-19.73	-47.7	12.01	2.46
313		-19.95			1.94
323		-20.08			1.69

The negative values of Gibbs free energy changes revealed that the adsorption process of nickel on kaolin is spontaneous and thermodynamically favorable ($\Delta G^0 < 0$) [109]. Furthermore, the increase in the absolute value of Gibbs free energy ($|\Delta G°|\uparrow$) with increasing temperature ($T\uparrow$) indicated that the higher temperatures contributed to increasing in the driving force of adsorption [110]. The negative value of the change enthalpy indicated that this process is exothermic ($\Delta H° < 0$) [111] and the adsorption executed is physical [112]. The negative value of the entropy change showed that the randomness at the level of the solid/solution interface has decreased ($\Delta S° < 0$) [113]. This effect was probably due to the structural stability of the kaolin during the adsorption process.

The activation energy was determined based on the Arrhenius equation (Eq. (15)) [114]

$$\ln k = \ln A - \frac{E_a}{RT} \tag{15}$$

Since the adsorption was carried out in two stages, namely fast stage and slow stage, we determined the constant k by the following equation:

$$k = k_{Lag} \times K_b \tag{16}$$

where Ea is the activation energy, k_{Lag} is the constant pseudo-first-order kinetic equation (min^{-1}), k_b is the constant

of pseudo-second-order speed equation (min^{-1}), T is the absolute temperature (K) and A is the frequency factor. The value of the activation energy allowed us to confirm that the adsorption of nickel on kaolin is produced by the exclusive intervention of intermolecular forces (physical adsorption) [115].

Desorption Study

Recovery of metal ions from the sorbent loaded is a significant process for its reuse and also to avoid storing contaminated solids which will regenerate another kind of pollution.

In this context, we proceeded to the desorption of nickel from charged kaolin. The desorption rate was represented by Eq. (15).

$$desorption\ rate = \frac{q_{des}}{q_{ads}} \times 100 \tag{15}$$

where q_{ads} is the adsorbed quantity at equilibrium (mg g^{-1}) for cycle I and q_{ads} is the desorbed quantity at equilibrium (mg g^{-1}) of each cycle.

Figure 13 illustrates respectively effect of eluents and distilled Water on nickel desorption (Fig. 13a) and nickel desorption rate (Fig. 13b). Table 7 displays the performances of the adsorption/desorption processes of nickel on kaolin.
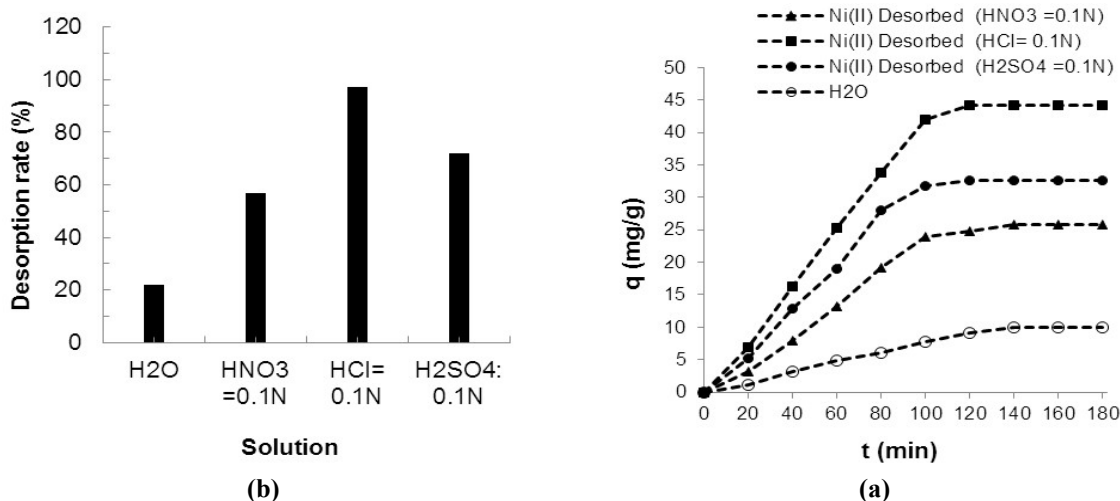

Fig. 13. Adsorption process: (a) desorption kinetics, (b) desorption rate.

Table 7. Adsorption and Desorption Performance of Nickel on Kaolin after 60 min

	qe $_{ads}$ (mg g^{-1})	qe $_{des}$ (mg g^{-1})	Desorption rate (%)
Cycle I	45.39	44.16	97.29
Cycle II	45.32	44.11	97.17
Cycle III	44.81	43.77	96.43
Cycle IV	39.67	34.21	75.63
Cycle V	34.24	30.12	66.35

Experimental tests performed indicated that the process of nickel ion desorption from saturated kaolin was better with HCl. at 0.1 N. Indeed, the calculated desorption rate is 97.2% (HCl), 71.9 % (H_2SO_4), 56.68 (HNO_3) and 22.11% (H_2O). For the rest of the study, HCl was chosen as the regeneration eluent and it was utilized over several adsorption/desorption cycles.

The experimental data indicated that the first 3 cycles of the 05 cycles realized are favorable. On the other hand, for the last two cycles, there was a decrease in the yield from 97.29 at 75.63% and 97.29 at 66.35%. The decrease in the desorption rate is probably due to the loss of mass of the adsorbent [116]. From its various investigations, it was concluded that kaolin could be reused over three successive cycles since it had retained almost its initial adsorption capacity.

CONCLUSIONS

In this work, the valorization of kaolin as a solid adsorbent was explored. Physico-chemical identification revealed that it consists largely of alumina, silica and a small amount of oxides. The morphological study showed the existence of a smooth surface caused by the stacking of sheets for raw kaolin. On the other hand for the activated form, it was noticed the existence of a more porous structure and the expansion of the surface under the effect of HCl.

The application of the theory of Brunauer, Emmett and Teller (BET) indicated that the specific surface area of raw and activated kaolin correspond respectively to 98 m^2 g^{-1} and 310 m^2 g^{-1}. The PZC study of kaolin showed that the pH corresponding to the point of zero load is 3.1.

From experimental results, it has been indicated that the adsorption of nickel on kaolin is feasible. The performance of this process (yield = 89.3%) was achieved after 60 min of agitation under specific operating conditions, namely V$_{ag}$: 150 rpm; pH: 4.3; T: 20 °C; Øs: 200 µm, M: 1 g, V: 1 l. Saturation of the kaolin was obtained after 60 minutes of stirring. The maximum adsorbed quantity of nickel by the kaolin in solution was measured at 45.39 mg g^{-1}.

The adsorption kinetics study indicated that this process is best described by the pseudo-first-order kinetic model. By cons, the data from the adsorption isotherms showed that the elimination of nickel is best adapted to the Langmuir model. This observation shows that the adsorption was carried out on a monolayer and homogeneous surface. Moreover, the study of the nickel transfer mechanism from the solution to the adsorbent has shown that the adsorption process is primarily controlled by external transport, which is an instantaneous process followed by diffusion in the pores. The thermodynamic study demonstrated that this process is spontaneous, thermodynamically feasible, and exothermic and nickel elimination had no effect on the structure of kaolin. The activation energy showed that the nickel elimination on the kaolin in solution is physical adsorption. The desorption process indicated that the saturated kaolin could be reused over three successive cycles because it had retained almost all of its initial adsorption capacity.

ACKNOWLEDGEMENTS

REFERENCES

[1] M. Karamipour, S. Fathi, M. Safari, Int. J. Environ. Anal. Chem. 10 (2021) 1915299.

[2] R. Katiyar, A. Kumar Patel, T.-B. Nguyen, R.R. Singhania, C.-W. Chen, C.-D. Dong, Bioresour. Technol. 328 (2021) 124829.

[3] K.P. Wasantha Lankathilaka, M. Rohini, M.M.M.G.P.G. Mantilaka, K.M. Nalin de Silva, Groundw. Sustain. Dev. 14 (2021) 100606.

[4] S. Andrejkovičova, A. Sudagar, J. Rocha, C. Patinha,

W. Hajjaji, E.F. da Silva A., Velosa, F. Rocha, Appl. Clay Sci. 126 (2016) 141.

[5] A.L. Pedrosa Xavier, O.F. Herrera Adarme, L.M. Furtado, G.M.D. Ferreira, L.H. Mendes da Silva, L.F. Gil, L.V. Alves Gurgel, J. Colloid Interface Sci. 516 (2018) 431.

[6] S. Markovic, A. Liang, S.B. Watson, D. Depew, A. Zastepa, P. Surana, J.V. Byllaardt, G. Arhonditsis, M. Dittrich, Environ. Poll. 252 (2019) 697.

[7] M.O. Awaleh, Y.D. Soubaneh, Hydrol. Curr. Res. 5 (2014) 164.

[8] A.S. Ayangbenro, O.O. Babalola, Int. J. Environ. Res. Public Health 14 (2017) 94.

[9] Y. Öztürk, Z. Ekmekçi, Miner. Eng. 159 (2020) 106613.

[10] J. Saien, M. Razi Asrami, Chem. Eng. Res. Des. 166 (2021) 259.

[11] M. Safari, Y. Yamini, Talanta 221 (2021) 121648.

[12] M. Hazrati, M. Safari, Environ. Prog. Sustainable Energy (2020) e13411.

[13] M. Karamipour, S. Fathi, M. Safari, Int. J. Environ. Anal. Chem. 191 (2021) 5299.

[14] R. El Kaim Billah, F. El Bachraoui, B. El Ibrahimi, H. Abou Oualid, Z. Kassab, G. Giacoman-Vallejos, M. Sillanpaa, M. Agunaou, A. Soufiane, Y. Abdellaoui, J. Solid State Chem. 310 (2022) 123023.

[15] B. Taraba, P. Bulavová, J. Chem. Thermodyn. 116 (2018) 97.

[16] F. Golmohammadi, M. Hazrati, M. Safari, Microchem. J. 144 (2019) 64.

[17] M. Samimi, M. Safari, Environ. Prog. Sustain. Energy (2022) 10.1002/ep.13859.

[18] R. Wang, Q. Yan, P. Su, J. Shu, M. Chen, Z. Xiao, Y. Han, Z. Cheng, Process Saf. Environ. Prot. 144 (2020) 366.

[19] X.J. Sun, H. Luo, Sustainability 6 (2014) 5820.

[20] F.F. Palermo, W.E. Risso, J.D. Simonato, C.B.R. Martinez, Ecotoxicol. Environ. Saf. 116 (2015) 9.

[21] M.M. Montazer-Rahmati, P. Rabbani, A. Abdolali, A.R. Keshtkar, J. Hazard. Mater. 185 (2011) 401.

[22] H. Parab, S. Joshi, N. Shenoy, A. Lali, U.S. Sarma, M. Sudersanan, Proc. Biochem. 41 (2006) 609.

[23] B. Ba Mohammed, A. Hsini, Y. Abdellaoui, H. Abou Oualid, M. Laabd, M. El Ouardi, A. Ait Addi, K. Yamni, N. Tijani, J. Environ. Chem. Eng. 8 (2020) 104419.

[24] M.N. Zafar, I. Aslam, R. Nadeem, S. Munir, U.A. Rana, S.-D. Khan, J. Taiwan Inst. Chem. Eng. 46 (2015) 82.

[25] A. Keranen, T. Leiviska, A. Salakka, J. Tanskanen, Desalination Water Treat. 53 (2015) 2645.

[26] E.Ç. Salihi, J. Wang, D.J.L. Coleman, L. Šiller, Sep. Sci. Technol. 51 (2016) 1317.

[27] J.J. Jacob, R. Varalakshmi, S. Gargi, M.A. Jayasri, K. Suthindhiran, Npj Clean. Water 1 (2018) 1.

[28] H. Wang, W. Wang, Y. Zhao, Z. Xu, L. Chen, L. Zhao, X. Tiana, W. Suna, RSC Adv. 8 (2018) 7899.

[29] M. Hernández Rodiguez, J. Yperman, R. Carleer, J. Maggen, D. Dadi, G. Gryglewicz, B.V. der Bruggen, J.F. Hernández, A.O. Calvis, J. Environ. Chem. Eng. 6 (2018) 1161.

[30] H. Hasar, J. Hazard. Mater. 97 (2003) 49.

[31] D. Nabarlatz, J. de Celis, P. Bonelli, A.L. Cukierman, J. Environ. Manag. 97 (2012) 109.

[32] Z.N. Garba, N.I. Ugbaga, A.K. Abdullahib, Beni-Suef Univ. J. Basic Appl. Sci. 5 (2016) 170.

[33] M. Irannajad, H.K. Haghighi, Clays Clay Miner. 65 (2017) 52.

[34] S. Ranasinghe, A.N. Navaratne, N. Priyantha, J. Environ. Chem. Eng. 6 (2018) 5670.

[35] S. Sobhanardakani, R.Z. Pak, M. Mohammadi, J. Arch. Hyg. Sci. 5 (2016) 47.

[36] M.K. Uddin, Chem. Eng. J. 308 (2016) 438.

[37] A. Kumar, P. Lingfa, Mater. Today: Proc. 22 (2020) 737.

[38] T. Chouchane, M. Yahi, A. Boukari, A. Balaska, S. Chouchane, J. Mater. Environ. Sci. 7 (2016) 2825.

[39] P.E. Dim, S.C. Olu, J.O. Okafor, J. Chem. Technol. Metall. 55 (2020) 1057.

[40] R. Mudzielwana, M.W. Gitari, P. Ndungu, Heliyon 5 (2019) e02756.

[41] D.M. El-Mekkawi, M.M. Selim, J. Environ. Chem. Eng. 2 (2014) 723.

[42] L. Mouni, L. Belkhiri, J.-C. Bollinger, A. Bouzaza, A. Assadi, A. Tirri, F. Dahmoune, K. Madani, H. Remini, Appl. Clay Sci. 153 (2018) 38.

[43] S. Wanga, L. Alaghaa, Z. Xu, Colloids Surf. A: Physicochem. Eng. Asp. 453 (2014) 13.

[44] S.M. Lee, D. Tiwari, Appl. Clay Sci. 59-60 (2012) 84.

[45] S. Sen Gupta, K.G. Bhattacharyya, J. Environ. Manag. 87 (2008) 46.

[46] E.I. Unuabonah, K.O. Adebowale, B.I. Olu-Owolabi, J. Hazard. Mater. 144 (2007) 386.

[47] M.-Q. Jiang, Q.-P. Wang, X.-Y. Jin, Z.-L. Chen, J. Hazard. Mater. 170 (2009) 332.

[48] M. Khairya, H.A. Ayoub, F.A. Rashwan, H.F. Abdel-Hafeza, Appl. Clay Sci. 153 (2018) 124.

[49] E.I. Unuabonah, B.I. Olu-owolabi, D. Okoro, K.O. Adebowale, J. Hazard. Mater. 171 (2009) 215.

[50] E.I. Unuabonah, K.O. Adebowale, B.I. Olu-Owolabi, L.Z. Yang, L.X. Kong, Hydrometallurgy 93 (2008) 1.

[51] X. Zhang, S. Lin, X.-Q. Lu, Z.-L. Chen, Chem. Eng. J. 163 (2010) 243.

[52] U.O. Aroke, A. Abdulkarim, R.O. Ogubunka, ATBU J. Environ. Technol. 6 (2013) 42.

[53] S. Mustapha, M.M. Ndamitso, A.S. Abdulkareem, J.O. Tijani, A.K. Mohammed, D.T. Shuai, Heliyon 5 (2019) e02923.

[54] S. Brunauer, P.H. Emmet, E. Teller, J. Amer. Chem. Soc. 60 (1938) 309.

[55] P.E. Dim, L.S. Mustapha, M. Termtanun, J.O. Okafor, Arab. J. Chem. 14 (2021) 103064.

[56] Z. Esvandi, R. Foroutan, S.J. Peighambardoust, B. Ramavandi, A. Akbari, Surf. Interfaces 21 (2020) 100754.

[57] J.S. Noh, J.A. Schwarz, J. Colloid Interfaces Sci. 130 (189) 157.

[58] A.H. Zyoud, A. Zubi, S.H. Zyoud, H.S. Hilal, S. Zyoud, N. Qamhieh, A. Hajamohideen, H.S. Hilal, Appl. Clay Sci. 182 (2019) 105294.

[59] P. Chutia, S. Kato, T. Kojima, S. Satokawa, J. Hazard. Mater. 162 (2009) 440.

[60] T. Chouchane, A. Boukari, Eng. Technol. J. 5(2020) 676. |

[61] S. Kumar, A.K. Panda, R.K. Singh, Bullet. Chem. React. Eng. Catal. 8 (2013) 61.

[62] R. Elmoubarki, F.Z. Mahjoubi, H. Tounsadi, J. Moustadraf, M. Abdennouri, A. Zouhri, A. ElAlban, N. Barka, Water Resour. Ind. 9 (2015) 16.

[63] F.S. Nworie, F.I. Nwabue, W. Otia, N.O. Omaka, H. Igwe, Anal. Bioanal. Chem. Res. 8 (2020) 91.

[64] G. K.Sarma, S.S. Gupta, K.G. Bhattacharyya, J. Environ. Manag. 171 (2016) 1.

[65] A. Labidi, A.M. Salaberria, S.C.M. Fernandes, J. Labidi, M. Abderrabba, J. Tai. Inst. Chem. Eng. 65 (2016) 140.

[66] T.V. Bauer, T.M. Minkina, D.L. Pinskii, S.S. Mandzhieva, S.N. Sushkova J. Geochem. Explor. 176 (2017) 108.

[67] A.S. Amina; S.S. Hussien; W.A. Hafez, O.A. Desouky, Egypt. J. Chem. 64 (2021) 6623.

[68] E.S. Penido, L.C.A. Melo, L.R.G. Guilherme, M.L. Bianchi, Sci. Total Environ. 671 (2019) 1134.

[69] E.R. Guerra, J. Aristizabal, B. Arce, E. Zurob, G. Dennett, R. Fuentes, A.V. Suescún, L. Cardenas, T.H. Rodrigues da Cunha, R.Cabezas, C.García-Herrera, C. Parra, J. Environ. Chem. Eng. 9 (2021) 105269.

[70] L. Mangaleshwaran, A. Thirulogachandar, V. Rajasekar, C. Muthukumaran, K. Rasappan, J. Taiwan Inst. Chem. Eng. 55 (2015) 112.

[71] M. Wiśniewska, K. Szewczuk-Karpisz, I. Ostolska, Fluid Ph Equilibria 360 (2013) 10.

[72] T.M. Berhane, J. Levy, P.S. Krekeler Mark, N.D. Danielson, Appl. Clay Sci. 132-133 (2016) 518.

[73] H. Zhao, X.K. Ouyang, L.Y. Yang, J. Mol. Liq. 324 (2021) 115122.

[74] C. Hu, P. Zhu, M. Cai, H. Hu, Q. Fu, Appl. Clay Sci. 143 (2017) 320.

[75] W.S. Wan Ngah, M.A.K.M. Hanafiah, Biochem. Eng. J. 39 (2008) 521.

[76] M. Sekar, V. Sakthi, S. Rengaraj, J. Colloid. Interface Sci. 279 (2004) 307.

[77] Y. Matsui, S. Nakao, A. Sakamoto, T. Taniguchi, N. Shirasaki, Water Res. 85 (2015) 95.

[78] B. Chen, W. Sun, C. Wang, X. Guo, Chem. Eng. J. 316 (2017) 160.

[79] M. Sekar, V. Sakthi, S. Rengaraj, J. Colloid Interface Sci. 279 (2004) 307.

[80] T. Kekes, G. Kolliopoulos, C. Tzia, J. Environ. Chem. Eng. 9 (2021) 105581.

[81] M. El Aassar, H. Fakhry, A.A. Elzain, H. Farouk, E.E. Hafez, Int. J. Biol. Macromol. 120 (2018) 1508.

[82] M.R. El Aassar, M.S. Masoud, M.F. Elkady, A.A. Elzain, Adv. Polym. Technol. 37 (2017) 2021.

[83] H. Freundlich, Z. Phys. Chem. 57 (1906) 385.

[84] Langmuir I., J. Am. Chem. Soc. 40 (1908) 361.

[85] S.M. Reddy Goddeti, M. Bhaumik, A. Maity, S. Sinha Ray, Int. J. Biol. Macromol. 149 (2020) 21.

[86] A.H. Shobier, M.M. El-Sadaawy, G.F. El-Said, Egypt. J. Aquat. Res. 46 (2020) 325.

[87] H. Zhuang, Y. Zhong, L. Yang, Chinese J. Chem. Eng. 28 (2020) 2758.

[88] F. Ayari, G. Manai, S. Khelifi, M. Trabelsi-Ayadi, J. Saudi Chem. Soc. 23 (2019) 294.

[89] T.W. Weber, R.K. Chakravorti, AICHE J. 20 (1974) 228.

[90] R. Dubey, J. Bajpai, A.K. Bajpai, Environ. Nanotechnol. Monit. Manag. 6 (2016) 32.

[91] R. Mudzielwana, M.W. Gitari, P. Ndungu, Heliyon 5 (2019) e02756

[92] S. Lagergren, Handlingar 24 (1898) 1.

[93] M. Haerifar, S. Azizian, J. Phys. Chem. C 118 (2014) 1129.

[94] W.J. Weber, J.C. Morris, J. Sanit. Eng. Div. Am. Soc. Civ. Eng. 89 (1963) 31.

[95] A.T. Mohd Din, B.H. Hameed, A.L. Ahmad, J. Hazard. Mater. 161 (2009) 1522.

[96] Z. Yu, W. Song, J. Li, Q. Li, Arab. J. Chem. 13 (2020) 4811.

[97] H. Demiral, G. Gündüzo-Glu, Bioresour. Technol. 101 (2010) 1675.

[98] A.E. Ofomaja, Bioresour. Technol. 101 (2010) 5868.

[99] D.M. Nevshia, A. Santianes, V. Munoz, A. Guerrero-Ruizi, Carbon 37 (1999) 1065.

[100] T.A. Saleh, Desalination Water Treat. 57 (2015) 1.

[101] W.H. Cheung, Y.S. Szeto, G. McKay, Bioresour. Technol. 98 (2007) 2897.

[102] R. Goswami, J. Shim, S. Deka, D. Kumari, R. Kataki, M. Kumar, Ecol. Eng. 97 (2016) 444.

[103] P. Liu, D. Rao, L. Zoua, Y. Teng, H. Yua, Sci. Total Envir. 767 (2021) 145447

[104] T. Chouchane, O. Khireddine, A. Boukari, J. Eng. Appl. Sci. 68 (2021) 00039.

[105] D.C. Ong, B.S. Mae, P. Ong, C.-C. Kan, M.D.G. de Luna, J. Clean. Prod. 190 (2018) 443.

[106] E.N. Zare, M.M. Lakouraj, M. Masoumi, Desalination Water Treat. 106 (2018) 209.

[107] S. Javidnezhad, A. Larki, Y. Nikpour, S.J. Saghanezhad, Anal. Bioanal. Chem. Res. 5 (2018) 217.

[108] R. Pelalak, Z. Heidari, S.M. Khatami, T.A. Kurniawan, A. Marjani, S. Shirazian, Arab. J. Chem. 14 (2021) 102991.

[109] M. Fayazia, M.A. Taherc, D. Afzalid, A. Mostafavic, Anal. Bioanal. Chem. Res. 2 (2015) 73.

[110] X. Yuan, Y. Wang, J. Wang, C. Zhou, Q. Tang, X. Rao, Chem. Eng. J. 221 (2013) 204.

[111] M. Torab-Mostaedi, H. Ghassabzadeh, M. Ghannadi-Maragheh, S.J. Ahmadi, H. Taher, Braz. J. Chem. Eng. 27 (2010) 66322010000200008.

[112] A. Marsh, A. Heath, P. Patureau, M. Evernden, P. Walker, Appl. Clay Sci. 166 (2018) 250.

[113] Y. Shi, T. Zhang, H. Ren, A. Kruse, R. Cui, Bioresour. Technol. 247 (2016) 370.

[114] F.-X. Chen, C.-R. Zhou, G.-P. Li, F.-F.Peng, Arab. J. Chem. 9 (2016) S1665.

[115] M. Zhang, Q. Yao, C. Lu, Z. Li, W. Wang, ACS Appl. Mater. Interfaces 6 (2014) 20225.

[116] E. Igberase, P. Osifo, A. Ofomaja, J. Environ. Chem. Eng. 2 (2014) 362.